The Astrophysical Journal, 690:L130–L134, 2009 January 10 doi:10.1088/0004-637X/690/2/L130

DETECTION OF C I IN ABSORPTION TOWARD PKS 1830−211 WITH THE eSMA

Sandrine Bottinelli[1], A. Meredith Hughes[2], Ewine F. van Dishoeck[1,3], Ken H. Young[2], Richard Chamberlin[4], Remo P. J. Tilanus[5,6], Mark A. Gurwell[2], David J. Wilner[2], Huib Jan van Langevelde[1,7], Michiel R. Hogerheijde[1], Robert D. Christensen[8], Hiroko Shinnaga[4], and Hiroshige Yoshida[4]
[1] Leiden Observatory, Leiden University, P.O. Box 9513, NL 2300 RA Leiden, The Netherlands; sandrine@strw.leidenuniv.nl
[2] Harvard-Smithsonian Center for Astrophysics, MS 42, 60 Garden Street, Cambridge, MA 02138, USA
[3] Max-Planck-Institut für Extraterrestrische Physik, Postfach 1312, 85741 Garching, Germany
[4] Caltech Submillimeter Observatory Office, 111 Nowelo St., Hilo HI 96720, USA
[5] Joint Astronomy Center, 660 N. A'ohoku Place, University Park, Hilo HI 96720, USA
[6] Netherlands Organisation for Scientific Research, Laan van Nieuw Oost-Indie 300, NL-2509 AC The Hague, The Netherlands
[7] Joint Institute for VLBI in Europe, Radiosterrenwacht Dwingeloo, Postbus 2, NL-7990 AA Dwingeloo, The Netherlands
[8] Harvard-Smithsonian Center for Astrophysics, Submillimeter Array, 645 North A'ohoku Place, Hilo HI 96721, USA
Received 2008 August 19; accepted 2008 November 23; published 2008 December 22

ABSTRACT

We report the first science observations and results obtained with the "extended" SMA (eSMA), which is composed of the SMA (Submillimeter Array), JCMT (James Clerk Maxwell Telescope), and CSO (Caltech Submillimeter Observatory). Redshifted absorptions at $z = 0.886$ of C I ($^3P_1$–$^3P_0$) were observed with the eSMA with an angular resolution of $0\farcs55 \times 0\farcs22$ at 1.1 mm toward the southwestern image of the remarkable lensed quasar PKS 1830−211, but not toward the northeastern component at a separation of $\sim 1''$. Additionally, SMA observations of CO, ^{13}CO, and C^{18}O (all $J = 4$–3) were obtained toward this object: CO was also detected toward the southwest component, but none of the isotopologues were. This is the first time [C I] has been detected in this object, allowing the first direct determination of relative abundances of neutral atomic carbon to CO in the molecular clouds of a spiral galaxy at $z > 0.1$. The [C I] and CO profiles can be decomposed into two and three velocity components, respectively. We derive C/CO column density ratios ranging from $\lesssim$0.5 (representative of dense cores) to $\sim$2.5 (close to translucent cloud values). This could indicate that we are seeing environments with different physical conditions or that we are witnessing the chemical evolution of regions where C has not completely been converted into CO.

Key words: galaxies: ISM – ISM: abundances – quasars: absorption lines – quasars: individual (PKS 1830)

1. INTRODUCTION

A powerful way to study the physical and chemical conditions in the interstellar medium (ISM) of distant galaxies is to observe chemical species in absorption against a strong continuum background source. Few such lines of sight have been unveiled so far but PKS 1830−211 (hereafter PKS 1830) is one of the most remarkable systems allowing this kind of study. PKS 1830 is a radio-loud quasar with a redshift of $z = 2.507$ (Lidman et al. 1999), for which millimeter continuum emission images show two compact components, northeast (NE) and southwest (SW), separated by $\sim 1''$ (Frye et al. 1997). This double structure represents two images of the background quasar, magnified and distorted by a lensing system at $z = 0.88582$ (Wiklind & Combes 1996). This lens was at first indirectly detected by the observations of broad H I and molecular absorptions at millimeter wavelengths (Wiklind & Combes 1996, 1998; Gérin et al. 1997; Muller et al. 2006). Wiklind & Combes (1998) suggested the lensing system to be an almost face-on spiral galaxy, which was recently confirmed by direct optical and infrared *Hubble Space Telescope* (*HST*) images (Courbin et al. 2002; Winn et al. 2002).

A key species in the physics and chemistry of the ISM in galaxies is atomic carbon. For instance, [C I] 492 GHz is one of the major far-infrared (FIR) fine-structure atomic lines via which cooling of the gas occurs (Hollenbach & Tielens 1997). Moreover, both C and C$^+$, which directly follow from C, are essential in radical reaction networks, especially those leading to carbon chains (Suzuki et al. 1992; Sternberg & Dalgarno 1995). Atomic carbon is also crucial for better understanding the structure of photodissociation regions (PDRs). Indeed, early observations of [C I] (e.g., Keene et al. 1985) revealed more intense emission than originally predicted by the models. Observations and theory now seem to have been reconciled by considering the effects of the clumpy structure of clouds (Hollenbach & Tielens 1997, and references therein).

Several studies have investigated the use of the neutral atomic carbon (C) to CO abundance ratio (N_C/N_{CO}) to investigate the physical conditions of the gas. A number of such analyses make use of UV absorption data, and hence are limited to diffuse clouds in our Galaxy. In order to measure N_C and N_{CO} in a dense environment, many studies have targeted submillimeter emission of these species. However, the lowest C transition lies at a rather high frequency ($^3P_1$ −^{3} P_0 at $\sim$492 GHz), and so its detection requires the use of ground-based facilities with sensitive receivers and/or a large collecting area, or the observation of a redshifted source. Moreover, in these submillimeter studies, the emission line data are averaged over large areas and suffer from radiative transfer and excitation effects (with a bias toward the densest regions). The eSMA ("extended" Submillimeter Array, Bottinelli et al. 2008) is particularly well suited for this kind of observation as it provides the high sensitivity and high spatial resolution required to observe the weak [C I] transition in PKS 1830. In this work, we present the first data obtained with the eSMA, which probe N_C/N_{CO} directly for the first time in absorption in the dense molecular regions of an external galaxy.

2. OBSERVATIONS AND DATA REDUCTION

2.1. eSMA and SMA Data

The eSMA consists of the SMA[9] array of eight 6 m antennas augmented by the nearby single dishes of the JCMT[10] (15 m) and the CSO[11] (10.4 m). The collecting area of the eSMA is twice that of the SMA alone, providing increased sensitivity, in particular for the longest baselines, which include the JCMT and CSO. Moreover, the longest baseline of the eSMA is increased by 50% compared to the SMA alone, which can bring the angular resolution down to below 0.″3 at 230 GHz, as reported here, and to below 0.″2 at 345 GHz, which will be the preferred frequency for eSMA observations.

Observations of PKS 1830 ($\alpha_{J2000} = 18^h33^m39^s.889$, $\delta_{J2000} = -21°03'39''.77$) were carried out with the eSMA for 7 hr on 2008 April 14 (with eight SMA antennas in the very extended configuration, or "vex"), and for 11 hr on 2008 August 5 with the SMA alone, also in vex configuration. The eSMA observations targeted the C I ($^3P_1-^3P_0$) transition while the SMA provided CO, ^{13}CO and C^{18}O (all $J = 4$–3) data. Table 1 summarizes the main observational parameters. The 45 eSMA baselines and the 28 SMA baselines had lengths ranging from 25–782 m (22–678 kλ) and 68–509 m (56–419 kλ), respectively, resulting in a best resolution at 1.1 mm of 0.″55 × 0.″22. The tracks interleaved 15–20 minute observations of PKS 1830 with 3–5 minute observations of the calibrators. Observations were carried out in single polarization mode with half-wave plates in the beam of the CSO and JCMT that automatically rotate to a common polarization as a function of elevation.

In this interim state of eSMA commissioning, the JCMT used receiver A3 which, due to a different intermediate frequency, provided a usable bandwidth of about 1.5 GHz, slightly less than the 2 GHz covered by the SMA and CSO. For both eSMA and SMA tracks, the correlator was setup to provide a uniform spectral resolution of 0.8125 MHz per channel across the full 1.5–2 GHz bandwith, resulting in 2304 to 3072 channels per baseline and velocity coverages of ∼1725 and ∼2450 km s^{-1}, for the eSMA and SMA, respectively. Weather conditions were poor on the two nights with atmospheric opacity at 225 GHz ranging from 0.15 to 0.25.

2.2. Data Reduction

The data were reduced and calibrated using the MIR/IDL software package,[12] and imaging was carried out with the MIRIAD software package. The SMA receiver temperatures ranged from ∼45 to 70 K on both nights, with the CSO comparable to the high end of this range, and the JCMT a factor of 2.5 times higher. The IF passband phase and amplitude were calibrated with observations of the strong sources 3C273, 3C454.3, J1924−292, and NRAO530 for the eSMA observations, and 3C273, 3C279 and 3C454.3 for the SMA-only data. Self-calibration of the eSMA phase of PKS 1830 was done on the shortest possible timescales using an initial model consisting of a pair of equal point sources separated by 1.″05 at a position angle of 42°. The amplitude gains for PKS 1830 were determined from the self-calibrated amplitudes of J1924−292. For the SMA-only data, phase calibration was performed in a standard way using J1733−130 to derive time-dependent amplitude gains throughout the night. The amplitude gains imply average efficiencies of about 0.75 for the SMA antennas, 0.70 for the JCMT, and 0.30 for the CSO; the low efficiency of the CSO is likely due to a known malfunction of its rotating polarizer. To set the flux scales, standard SMA monitoring observations of J1924−292 (eSMA) and 3C279 (SMA-only) at 230 GHz and 345 GHz were used (uncertainty $\lesssim$ 20%).

Table 1
Main Observational Parameters for PKS 1830

Parameter	DSB continuum	C ($^3P_1-^3P_0$)	^{12}CO(4-3)
ν_{rest} (GHz)[a]	...	492.16065	461.04077
ν_{obs} (GHz)[a]	1.1 mm	260.97965	244.47761
Channel width	2 × ∼1.5 GHz[b]	0.93 km s^{-1}[c]	0.99 km s^{-1}[c]
Beam FWHM	0.″55 × 0.″22	0.″62 × 0.″30	0.″57 × 0.″40
Beam P.A.	32°	38°	15°
Array	eSMA	eSMA	SMA

Notes.
[a] The rest and observing frequencies (ν_{rest} and ν_{obs}) are related by $\nu_{obs} = \nu_{rest}/(1+z)$, with $z = 0.88582$.
[b] Note that in the 230 GHz band, the eSMA bandwidth is limited by that of the JCMT's receiver A3; see the text for details.
[c] Corresponding to a uniform frequency resolution of ∼0.8 MHz.

3. RESULTS

The continuum map, obtained with the eSMA and derived from line-free channels, is displayed in Figure 1. This map shows the two lensed images of the distant quasar, separated by 1″, consistent with previously reported values. Figure 1 also shows the [C I] spectra at the peak of the continuum emission of the SW and NE components.

Figure 2 shows the absorption spectra of [C I] and CO (4 − 3) as a function of heliocentric velocity, V_{hel}, observed in the SW source by the eSMA and SMA, respectively. Two- and three-component Gaussian fits were applied to the [C I] and CO spectra, respectively, and are overplotted on Figure 2. Our [C I] velocities and widths agree within the errors with those reported for other molecular species (Muller et al. 2006; Menten et al. 2008) and these values were used to guide the fits to the blended CO components. The presence of a fourth velocity component at ∼+20 km s^{-1} in the CO spectrum is possible, but was not fitted due to its low signal-to-noise ratio and is therefore not investigated further in this work. The derived parameters are given in Columns 2–5 of Table 2. The optical depths at velocities $V_{hel,0}$ were derived using $\tau_0 = -\ln(F_{V_{hel,0}}/F_c)$, where $F_{V_{hel,0}}$ and F_c are the line and continuum fluxes, respectively. This equation implicitly assumes that the covering factor f_c of the absorbing molecular gas across the finite extent of the background continuum source is 1, which will be discussed in Section 4.

Using line data from LAMDA, the Leiden Atomic and Molecular Database,[13] we ran the radiative transfer code RADEX (van der Tak et al. 2007) for a range of H_2 number densities n and kinetic temperatures T_{kin}, and for $T_{CMB} = 5.16$ K; we obtain the

[9] The Submillimeter Array is a joint project between the Smithsonian Astrophysical Observatory and the Academia Sinica Institute of Astronomy and Astrophysics and is funded by the Smithsonian Institution and the Academia Sinica.
[10] The James Clerk Maxwell Telescope is operated by The Joint Astronomy Centre on behalf of the Science and Technology Facilities Council of the United Kingdom, the Netherlands Organisation for Scientific Research, and the National Research Council of Canada.
[11] The Caltech Submillimeter Observatory is supported by grant number AST-0540882 from the National Science Foundation.
[12] http://cfa-www.harvard.edu/∼cqi/mircook.html
[13] http://www.strw.leidenuniv.nl/∼moldata/

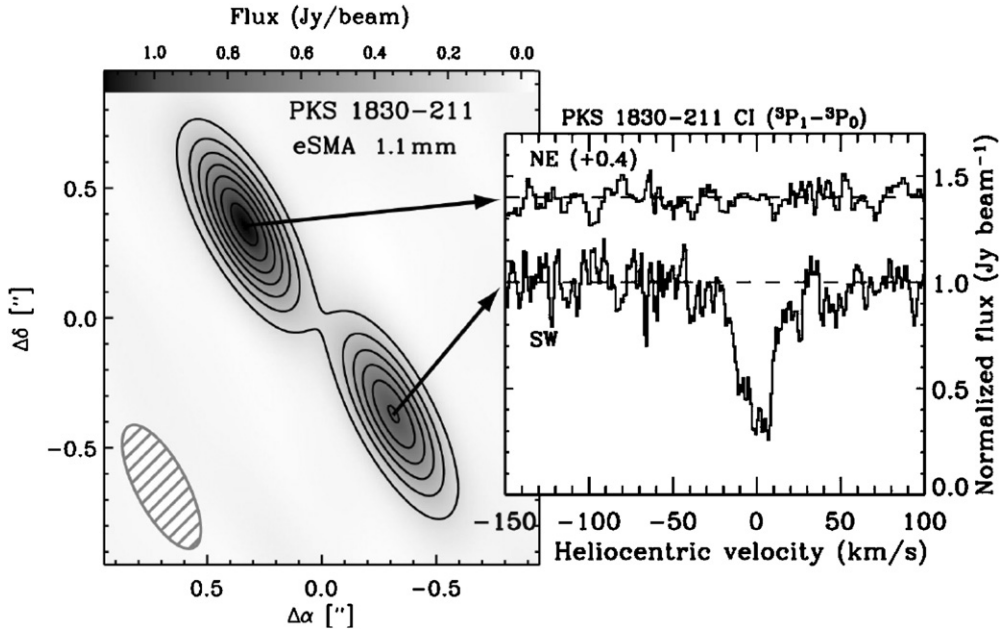

Figure 1. eSMA 1.1 mm continuum map and [C I] spectra of PKS 1830. Absolute astrometry information is lost during the self-calibration process, so that the offsets here are relative to the center of the double point source. The contour levels are multiples of 150 mJy. The $0\farcs55 \times 0\farcs22$ beam is shown in the lower left corner.

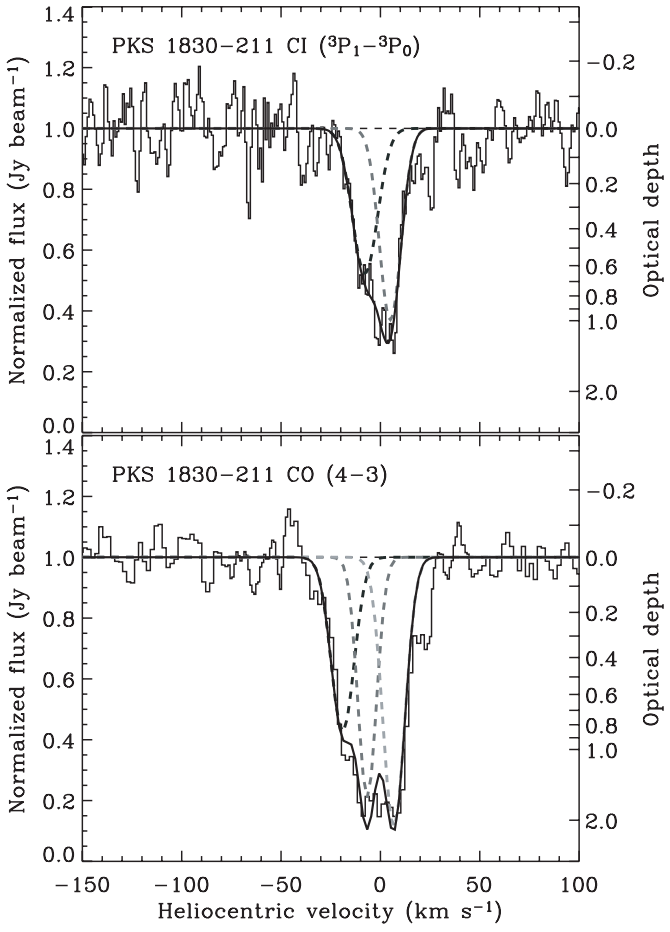

Figure 2. eSMA spectrum of C I ($^3P_1 - ^3P_0$) and SMA spectrum of CO ($J = 4 - 3$) observed toward the SW component. Spectra were smoothed to a velocity resolution of 2.8 and 5.9 km s^{-1}, yielding rms before normalization of 0.07 and 0.04 Jy beam^{-1}, corresponding to 0.09 and 0.05 on optical depth scale, for [C I] and CO, respectively. Overlaid in dashed lines are two- and three-component Gaussian fits to the [C I] and CO profiles, respectively, while the solid lines are the sum of these individual components.

Table 2
Observed and Derived Line Parameters for the SW Component

Transition	$V_{hel,0}$ (km s^{-1})	τ_0	FWHM (km s^{-1})	$\int \tau dV$ (km s^{-1})	N[a] (10^{17} cm^{-2})	N_C / N_{CO}
[C I]	−19.0	<0.15[c]	10.0[d]	<1.6	<1.6	<0.6
	−7.8	0.65	15.1	10.3	$10.2^{+4.5}_{-4.4}$	$2.7^{+0.5}_{-2.0}$
	5.0	0.99	12.9	13.6	$13.5^{+6.0}_{-5.8}$	$2.2^{+0.4}_{-1.6}$
CO	−19.0[b]	0.86	13.7	12.5	$2.6^{+10.9}_{-1.3}$	···
	−6.5[b]	1.59	11.0[b]	18.6	$3.8^{+16.2}_{-1.9}$	···
	6.9[b]	2.21	13.0[b]	30.6	$6.2^{+27.1}_{-3.2}$	···
^{13}CO, C^{18}O	···	<0.1[c]	10.0[d]	<1.1	<0.2	···

Notes.
[a] Using $T_{ex} = 10^{+10}_{-4}$ K for CO, ^{13}CO, C^{18}O, and 15^{+10}_{-7} K for C I.
[b] These positions/FWHM were constrained to the positions obtained from the fit to the C I transition (within the errors) and/or to the positions/FWHM obtained by Muller et al. (2006).
[c] 2σ upper limit in the ∼6 km s^{-1} channel.
[d] Fixed.

excitation temperature for each (n, T_{kin}), and hence determine (n, T_{kin}) ∼ (0.2–5 × 10^4 cm^{-3}, 10–30 K) corresponding to the excitation temperature $T_{ex} = T_{rot} \sim 5.2$–8 K derived by Muller et al. (2006) and Wiklind & Combes (1996) for molecular diagnostics of the physical conditions of dense cores such as HCO$^+$. Using these same (n, T_{kin}), we in turn obtain T_{ex} for CO and C of ∼6–20 and 8–25 K. These slightly higher T_{ex} values are consistent with the lower Einstein A-coefficients of CO and C compared to HCO$^+$. N_{CO} and N_C are then computed from, e.g., Equation (2) of Muller et al. (2006), and are given in Table 2. The largest N_C is consistent with the upper limit of ∼10^{18} cm^{-2} reported by Gérin et al. (1997), and the CO column density we obtain for the ∼7 km s^{-1} component, $0.9^{+3.9}_{-0.5} \times 10^{18}$ cm^{-2}, is also in agreement with the estimate given by these authors. Our results yield $N_C/N_{CO} \sim 2.5$ for the two components at $V_{hel,0} \sim -7$ and ∼6 km s^{-1}, and an upper limit of ∼0.5 for the third component at $V_{hel,0} \sim -19$ km s^{-1}.

Finally, we derived an upper limit on N_{CO} in the NE component of $\lesssim 3.5 \times 10^{16}$ cm^{-2}, assuming a line width of 15 km s^{-1} (Muller et al. 2006). This is consistent with the smallest N_{CO} of 3×10^{16} cm^{-2} expected from the range of HCO^+ to CO column density ratios determined from our data and that of Muller et al. (2006). Nondetection of the targeted molecules in the NE component could be due to the change in absorption reported by Muller & Guélin (2008) in this source.

4. DISCUSSION AND CONCLUSION

Observations of C, C^+, and CO can be used to probe the physical conditions of the gas. However, studies of the (clumpy) interstellar medium in external galaxies are complicated by several issues: (1) the large observing beams which encompass several regions of differing conditions; (2) the difficulty of performing [C I] observations due to the weakness of the lines and the poorer atmospheric transparency at the high frequencies of the [C I] transitions (492 and 809 GHz); and (3) the impossibility of accessing the [C II] 158-μm transition from the ground. The observations presented here make it possible to tackle the first two points. Indeed, since the lines are detected in absorption and the galaxy responsible for the latter is almost face-on, the line profiles will not be much affected by rotation broadening. Regarding point (2), it is worthwhile to note that, in fact, no [C I] absorption has yet been detected in a local galaxy at $z \sim 0$. For PKS 1830, the absorbing material is at a redshift of ~0.89, shifting the 492-GHz [C I] line to ~261 GHz where the atmosphere is more transparent and stable.

While absorption data circumvent some of the problems inherent to emission spectra, some limitations unfortunately remain, in particular, our (lack of) knowledge of the structure of the absorbing gas. This translates partly into the estimation of the covering factor f_c, which is one of the major sources of uncertainty (along with T_{ex}) in the determination of the column densities. For CO(4−3), the largest optical depth is ~2, meaning that the absorption almost reaches zero intensity, but it is not heavily saturated as indicated by the nondetection of the less abundant ^{13}CO. Indeed, Muller et al. (2006) derive $^{12}C/^{13}C$ ~27, so that if CO were heavily saturated, the expected optical depth of ^{13}CO would be $\gtrsim 0.1$, i.e., at the 2σ detection limit. Hence, the covering factor of the absorbing material must be close to unity, as noted by previous studies of this source. This is consistent with the picture of individual clouds with sizes of order ~1 pc (see Menten et al. 1999; Muller & Guélin 2008, and sizes of typical Galactic molecular clouds of up to a few pc) in front of a background source of projected size $\lesssim 1$ pc at the distance of the galaxy, corresponding to the deconvolved core size of ~0.228 × 0.148 mas measured by Jin et al. (2003) for the SW image of PKS 1830 at 7 mm with the VLBA.

Comparing the total H column density derived with different methods can indicate whether the "cloud" is uniform (e.g., Wiklind & Combes 1997). For the SW source, there is no strong evidence for clumpiness, since, in this case, the total H column density derived from X-ray data (~3.5×10^{22}cm^{-2}, Mathur & Nair 1997) is comparable to that derived from millimeter CO absorption (~5×10^{22} cm^{-2}, assuming $CO/H_2 \sim 5 \times 10^{-5}$), or from C I absorption (~6×10^{22} cm^{-2}, assuming a typical $C/H_2 \sim 8 \times 10^{-5}$, Frerking et al. 1989). Hence, the assumption that the individual velocity components consist of material with homogeneous physical and chemical conditions seems sufficient, which allows us to compare the column density ratios.

Our data indicate two types of N_C/N_{CO} (see Table 3 for comparisons): a low value, $\lesssim 0.5$, representative of dense cores or PDRs ($\lesssim$0.5–1), and a somewhat high value, ~2.5, close to those derived for translucent clouds (~3–6). Qualitatively, low N_C/N_{CO} are found in environments with low neutral atomic carbon abundances, such as high-UV environments (where C becomes ionized), or high-density environments (where CO formation is efficient). The presence of high density tracers such as HCO^+, HCN, and CS supports the latter case of a dense core for the $V_{hel} = -19$ km s^{-1} component. On the other hand, high N_C/N_{CO} are representative of low-density, low-column density, mild-UV environments where CO is photodissociated but atomic carbon is not ionized. For the $V_{hel} \sim -7$ km s^{-1} component, the detection of hot NH_3 ($V_{LSR} \sim 5$ km s^{-1}, Henkel et al. 2008) and large H I optical depth (e.g., Koopmans & de Bruyn 2005) point toward a low-density PDR. Since hot NH_3 was not detected at $V_{hel} \sim 5$ km s^{-1}, the high N_C/N_{CO} here more likely indicates diffuse or translucent conditions. An absorbing source at $z \sim 2.4$ with similar diffuse material, albeit a higher N_C/N_{CO} of ~10, was reported by Srianand et al. (2008).

Atomic C variations could also be explained by chemical evolution (Maezawa et al. 1999): since the timescale for conversion of C to CO is comparable to the dynamical timescale of a dense core (~10^6 yr), N_C/N_{CO} is expected to be high in the early stage of dense core formation and to decrease with time. Hence, our $N_C/N_{CO} \sim 2.5$ could be indicative of a cloud in an intermediate stage of evolution from diffuse to dense gas, where C has not completely converted into CO.

In conclusion, the data presented here demonstrate the ability of the eSMA to provide observers with high angular resolution, high sensitivity observations. Furthermore, they allowed us to investigate the physical and chemical conditions of the material obscuring the SW component of PKS 1830, and determine

Table 3
Comparison of N_C/N_{CO} Measurements

Source	N_C/N_{CO}	References
Translucent clouds	~3–6	Stark & van Dishoeck 1994
Diffuse clouds	~1–80	Federman et al. 1980
Diffuse material at $z = 2.418$	~10	Srianand et al. 2008
Molecular clouds		
Ophiucus	~0.05–1	Frerking et al. 1989
G34.3+0.2	~0.1–1	Little et al. 1994
W3, NCG2024, S140, Cep A	~0.1–0.5	Plume et al. 1999
TMC1, L1527	~0.06–0.25	Maezawa et al. 1999
Orion A/B (multi position)	0.05–0.21	Ikeda et al. 2002
PDRs (multi-positions)		
M17, S140; IC 348	0.02–0.25	Keene et al. 1985; Sun et al. 2008
NGC1977	0.03–0.2	Minchin & White 1995
Orion Bar	0.04–0.3	Jansen et al. 1995
S106	0.02–0.09	Schneider et al. 2003
IC 63 (high/low density)	0.1–0.7 / 2–3	Jansen et al. 1996
Galaxies		
M33 (4 positions)	0.03–0.16	Wilson 1997
IC 342 (center)	0.5–0.6	Israel & Baas 2003
NGC 253; Maffei 2 (center)	0.2–0.3	Israel et al. 1995; Israel & Baas 2003
M82	~0.5	White et al. 1994
M83 (5″, 5″)	~0.3	Petitpas & Wilson 1998
M83 (center), NGC 6946	~0.9	Israel & Baas 2001
M51 (center)	0.4–1.0	Israel et al. 2006
Spiral at $z = 0.886$	$\lesssim$0.5, ~2.5	This work

N_C/N_{CO} directly in a dense molecular cloud located at $z = 0.886$.

We are very much indebted to Ray Blundell, Gary Davis, and Tom Phillips, the directors of the SMA, JCMT, and CSO, respectively, for their continued support and without whom the eSMA would not be possible. The development of the eSMA has been facilitated by grant 614.061.416 from the Netherlands Organisation for Scientific Research, NWO. A.M.H. is supported by a National Science Foundation Graduate Research Fellowship.

REFERENCES

Bottinelli, S., et al. 2008, in SPIE Conf. on Astronomical Instrumentation (Bellingham, WA: SPIE)
Courbin, F., Meylan, G., Kneib, J.-P., & Lidman, C. 2002, ApJ, 575, 95
Federman, S. R., Glassgold, A. E., Jenkins, E. B., & Shaya, E. J. 1980, ApJ, 242, 545
Frerking, M. A., Keene, J., Blake, G. A., & Phillips, T. G. 1989, ApJ, 344, 311
Frye, B., Welch, W. J., & Broadhurst, T. 1997, ApJ, 478, L25
Gérin, M., Phillips, T. G., Benford, D. J., Young, K. H., Menten, K. M., & Frye, B. 1997, ApJ, 488, L31
Henkel, C., Braatz, J. A., Menten, K. M., & Ott, J. 2008, A&A, 485, 451
Hollenbach, D. J., & Tielens, A. G. G. M. 1997, ARA&A, 35, 179
Ikeda, M., Oka, T., Tatematsu, K., Sekimoto, Y., & Yamamoto, S. 2002, ApJS, 139, 467
Israel, F. P., & Baas, F. 2001, A&A, 371, 433
Israel, F. P., & Baas, F. 2003, A&A, 404, 495
Israel, F. P., Tilanus, R. P. J., & Baas, F. 2006, A&A, 445, 907
Israel, F. P., White, G. J., & Baas, F. 1995, A&A, 302, 343
Jansen, D. J., Spaans, M., Hogerheijde, M. R., & van Dishoeck, E. F. 1995, A&A, 303, 541
Jansen, D. J., van Dishoeck, E. F., Keene, J., Boreiko, R. T., & Betz, A. L. 1996, A&A, 309, 899
Jin, C., Garrett, M. A., Nair, S., Porcas, R. W., Patnaik, A. R., & Nan, R. 2003, MNRAS, 340, 1309
Keene, J., Blake, G. A., Phillips, T. G., Huggins, P. J., & Beichman, C. A. 1985, ApJ, 299, 967
Koopmans, L. V. E., & de Bruyn, A. G. 2005, MNRAS, 360, L6
Lidman, C., Courbin, F., Meylan, G., Broadhurst, T., Frye, B., & Welch, W. J. W. 1999, ApJ, 514, L57
Little, L. T., Gibb, A. G., Heaton, B. D., Ellison, B. N., & Claude, S. M. X. 1994, MNRAS, 271, 649
Maezawa, H., et al. 1999, ApJ, 524, L129
Mathur, S., & Nair, S. 1997, ApJ, 484, 140
Menten, K. M., Carilli, C. L., & Reid, M. J. 1999, in ASP Conf. Ser. 156, Highly Redshifted Radio Lines, ed. C. L. Carilli, S. J. E. Radford, K. M. Menten, & G. I. Langston (San Francisco, CA: ASP) 218
Menten, K. M., Guesten, R., Leurini, S., Thorwirth, S., Henkel, C., Klein, B., Carilli, C. L., & Reid, M. J. 2008, A&A, 492, 725
Minchin, N. R., & White, G. J. 1995, A&A, 302, L25+
Muller, S., & Guélin, M. 2008, A&A, 491, 739
Muller, S., Guélin, M., Dumke, M., Lucas, R., & Combes, F. 2006, A&A, 458, 417
Petitpas, G. R., & Wilson, C. D. 1998, ApJ, 503, 219
Plume, R., Jaffe, D. T., Tatematsu, K., Evans, N. J., & J., II, Keene 1999, ApJ, 512, 768
Schneider, N., Simon, R., Kramer, C., Kraemer, K., Stutzki, J., & Mookerjea, B. 2003, A&A, 406, 915
Srianand, R., Noterdaeme, P., Ledoux, C., & Petitjean, P. 2008, A&A, 482, L39
Stark, R., & van Dishoeck, E. F. 1994, A&A, 286, L43
Sternberg, A., & Dalgarno, A. 1995, ApJS, 99, 565
Sun, K., Ossenkopf, V., Kramer, C., Mookerjea, B., Röllig, M., Cubick, M., & Stutzki, J. 2008, A&A, 489, 207
Suzuki, H., Yamamoto, S., Ohishi, M., Kaifu, N., Ishikawa, S. I., Hirahara, Y., & Takano, S. 1992, ApJ, 392, 551
van der Tak, F. F. S., Black, J. H., Schöier, F. L., Jansen, D. J., & van Dishoeck, E. F. 2007, A&A, 468, 627
White, G. J., Ellison, B., Claude, S., Dent, W. R. F., & Matheson, D. N. 1994, A&A, 284, L23
Wiklind, T., & Combes, F. 1996, Nature, 379, 139
Wiklind, T., & Combes, F. 1997, A&A, 328, 48
Wiklind, T., & Combes, F. 1998, ApJ, 500, 129
Wilson, C. D. 1997, ApJ, 487, L49
Winn, J. N., Kochanek, C. S., McLeod, B. A., Falco, E. E., Impey, C. D., & Rix, H.-W. 2002, ApJ, 575, 103